

# A placement-value based approach to concave ROC analysis

Soutik Ghosal<sup>1</sup> and Zhen Chen<sup>\*2</sup>

<sup>1</sup>Division of Biostatistics, Public Health Sciences Department, School of Medicine, University of Virginia, Charlottesville, VA 22903

<sup>2</sup>Biostatistics and Bioinformatics Branch, Division of Intramural Population Health Research, *Eunice Kennedy Shriver* National Institute of Child Health and Human Development, Bethesda, MD 20892

## Abstract

The receiver operating characteristic (ROC) curve is an important graphic tool for evaluating a test in a wide range of disciplines. While useful, an ROC curve can cross the chance line, either by having an S-shape or a hook at the extreme specificity. These non-concave ROC curves are sub-optimal according to decision theory, as there are points that are superior than those corresponding to the portions below the chance line with either the same sensitivity or specificity. We extend the literature by proposing a novel placement value-based approach to ensure concave curvature of the ROC curve, and utilize Bayesian paradigm to make estimations under both a parametric and a semiparametric framework. We conduct extensive simulation studies to assess the performance of the proposed methodology under various scenarios, and apply it to a pancreatic cancer dataset.

**Key Words:** AUC; Placement values; concavity.

## 1 Introduction

The receiver operating characteristic (ROC) curve is a popular two-dimensional graphic tool to assess how a test of interest differentiates an affected and a reference population ([Birdsall, 1966](#); [Peterson et al., 1954](#)). It is constructed by plotting pairs of false positive and true positive rates across various thresholds of the test value. A useful summary measure based

---

\*zhen.chen@nih.gov

on the ROC curve analysis is the area under the ROC curve (AUC), which is a scalar between 0.5 and 1.0, with higher values for higher discrimination capacity of the test (McClish, 1989).

There is no inherent shape constraint on a ROC curve based on its definition, with the exception that it is monotonely nondecreasing. A ROC curve can be “S”-shaped. This can arise under the well-known Bi-Normal model with a considerable discrepancy in standard deviations between the affected and reference groups (Green et al., 1966), as illustrated in Figure 1a. A ROC curve may feature a discernible dip at higher specificity levels, exhibiting the so-called “hooks” phenomenon. Figure 1b depicts such an example that was obtained from a non-concave standard Bi-Normal model for assessing the diagnostic potential of the carbohydrate antigen CA199 for pancreatic cancer (Wieand et al., 1989). In both cases, the ROC curve features a portion below the chance line, suggesting that it is sub-optimal as there are always decision points that have better sensitivity or specificity.

These nonconcave ROC curve shapes are not uncommon in medical research and have been extensively discussed in the literature (Bandos et al., 2017; Hillis and Berbaum, 2011; Hillis, 2012). These symptoms are indicative of non-proper ROC curves that are usually based on a non-optimal decision rule. Recent literature advocates for the use of proper ROC curves (Egan, 1975; Metz and Pan, 1999) that ensure a concave shape curvature and interpretable sensitivity measures at any specificity level. Concave ROC curves have been proposed either by considering special distributions for the affected and reference test scores or by considering alternative decision variables. The former includes the Bi-Gamma model of Dorfman et al. (1996), the Bi-Lomax model of Campbell and Ratnaparkhi (1993), and the Bi-Beta model of Mossman and Peng (2016), among others. A common theme of these works is the use of some shared parameters in the affected and reference distributions to induce concavity. In the latter, the proper Bi-Normal model of Metz and Pan (1999) resorts to a likelihood ratio transformation of the test scores as a new decision variable; see also Hillis (2016) and Sacchetto and Gasparini (2018).

While the literature has addressed concavity in ROC analysis, existing methodologies are predominantly parametric, making them susceptible to model mis-specifications. This paper aims to bridge this gap by proposing alternative concave ROC models that are less sensitive to such mis-specifications. Our proposed approach leverages placement values (PV), a concept used by Pepe (2003) and others that makes use of standardization of affected test scores relative to the reference population. The advantage of the PV-based approach lies in its representation of the ROC curve as the distribution function of PVs. Recent extensions in this approach, pioneered by Cai and Pepe (2002); Cai (2004); Lin et al. (2012), enable semi-parametric and nonparametric modeling of ROC curves. To achieve concavity in the ROC curve, we adopt the PV-based approach and incorporate the concept of concave distribution functions introduced by Hansen and Lauritzen (2002). In essence, our approach expresses a ROC curve as the distribution function of PVs, and utilizes the concave distribution function concept to impose the desired concave shape of the distribution function through a mixture distribution. Furthermore, we present both parametric and semi-parametric frameworks of the proposed approach to accommodate complex scenarios effectively, and adopt a Bayesian perspective to facilitate the estimation and inference.

The rest of the article is organized as follows. Section 2 describes the detailed development

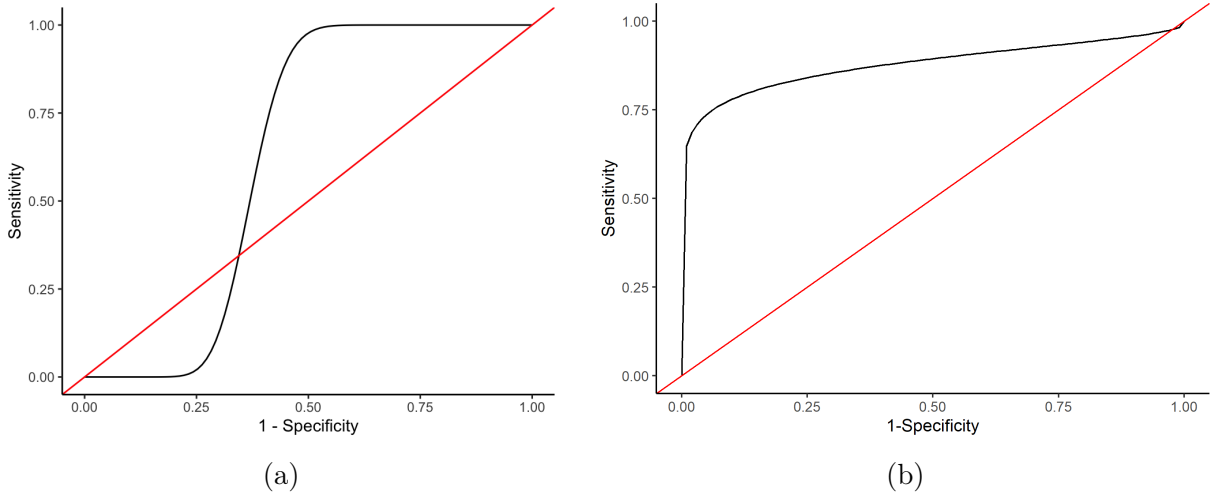


Figure 1: (a) An S-shaped ROC curve from a Bi-Normal model with unequal variances, (b) an ROC curve with a “hook”, “naïvely” estimated using the pancreatic cancer data detailed in Section 4. The red line is the chance line.

of the proposed approach, including model formulations and estimations by the Bayesian paradigm. Both parametric and semiparametric frameworks will be considered. Section 3 demonstrates the performance of the developed methodology through detailed simulation studies, and Section 4 presents a real data application that evaluates the diagnostic accuracy of carbohydrate antigen CA199 for pancreatic cancer. We conclude with a brief discussion in Section 5.

## 2 Modeling framework

### 2.1 Notations and background

A receiver operating characteristic curve is a graphical tool to assess the diagnostic ability of a test to discriminate two populations, say reference and affected (Pepe, 2003). Let 0 and 1 respectively be the status of the reference and affected populations, and let  $Y_i^0$  and  $Y_i^1$  be test scores of reference and affected subject  $i$  ( $i = 1, \dots, N$ , with the understanding that  $N$  can be different for the reference and affected populations). Let  $F_0$  and  $F_1$  be the corresponding cumulative distribution functions (CDF). Then the ROC curve is defined as

$$ROC(t) = 1 - F_1(F_0^{-1}(1 - t)), \quad t \in (0, 1). \quad (2.1)$$

The area under the ROC curve (AUC) is a measure that can be interpreted as the probability that a test score of an affected subject is higher than that of a reference subject (i.e.,  $P[Y_i^1 > Y_i^0]$ ) and is given as  $AUC = \int_0^1 ROC(t) dt$ .

Different parametric ROC models can be considered by varying  $F_0$  and  $F_1$ . The Bi-Normal (BN) model is a parametric approach with a normality assumption for affected and

reference test scores,

$$Y_i^1 \sim N(\mu_1, \sigma_1^2) \text{ and } Y_i^0 \sim N(\mu_0, \sigma_0^2).$$

The resultant ROC curve and AUC have closed-form expressions given by

$$ROC(t) = \Phi(a + b\Phi^{-1}(t)), \quad t \in (0, 1) \quad (2.2)$$

$$AUC = \Phi\left(\frac{a}{\sqrt{1+b^2}}\right), \quad (2.3)$$

where,

$$a = \frac{\mu_1 - \mu_0}{\sigma_1}, \quad b = \frac{\sigma_0}{\sigma_1},$$

and  $\Phi(\cdot)$  is the CDF of the standard normal distribution.

## 2.2 Placement value-based approaches

To seek a direct approach to estimating the ROC curve, Pepe and others (Pepe, 2003; Pepe and Cai, 2004; Cai, 2004; Lin et al., 2012) proposed to use placement values. A placement value (PV) is defined as the standardization of the test score from the affected population relative to that of the reference population:

$$z_i = 1 - F_0(Y_i^1).$$

In other words, PV  $z_i$  can be interpreted as the proportion of the reference population with scores more than that of affected score  $Y_i^1$ . It can be easily shown that the CDF of  $z_i$  (say,  $F_z$ ) is the ROC curve to discriminate reference and affected populations. As such, whereas we model  $Y_i^1$  and  $Y_i^0$  in the conventional approach of ROC analysis, we model  $z_i$  and  $Y_i^0$  in the PV-based approach.

## 2.3 Concave ROC curves

The aforementioned connection between ROC curve and CDF of the PV makes it possible to impose a concave curvature on the ROC curve. To that end, we borrow the idea of a concave CDF from Hansen and Lauritzen (2002) as stated below for completeness.

**Lemma 1** *A CDF  $F$  is concave if and only if there exists a distribution function  $G$  on the same support  $\Omega$  of  $F$  such that  $F$  admits the representation*

$$F(z) = \int F_w(z) dG(w), \quad z \in \Omega,$$

where  $F_w$  for  $w \neq 0$  is the distribution function corresponding to the uniform distribution on  $(0, w)$ , i.e.,

$$F_w(z) = \frac{1}{w} \min\{z, w\}.$$

Equivalently, this result can be stated as follows, which can aid the development of an efficient computational algorithm:

**Lemma 2** *Let  $F$  be the CDF of  $Z$ .  $F$  is concave if and only if  $Z$  can be written as  $Z = WV$  where  $W$  and  $V$  are independent,  $V \sim U(0, 1)$  and  $W$  has some distribution  $G$  on the same support of  $Z$ .*

It is immediate from Lemma 2 that  $AUC = 1 - E(W)/2$ . The essence of these results is simple: in order to model the distribution function  $F_z$  of  $z$ , we can model the distribution function  $G$  of  $w$ . Our strategy to model a concave ROC curve using  $\mathbf{z}$  therefore involves three steps:

1. Construct a hierarchical model

$$\begin{aligned} z_i | w_i &\sim U(0, w_i), \\ w_i | \boldsymbol{\delta} &\sim G(w_i | \boldsymbol{\delta}), \end{aligned}$$

where  $\boldsymbol{\delta}$  is the parameter vector indexing  $G$ .

2. Develop an MCMC algorithm to obtain a sample of  $\mathbf{w} = (\mathbf{w}^{(1)}, \dots, \mathbf{w}^{(L)})$  from the posterior distribution  $p(G | \mathbf{z})$ , where  $\mathbf{w}^{(l)} = (w_1^{(l)}, \dots, w_S^{(l)})$  is a sample of size  $S$  at the  $l^{\text{th}}$  iteration.
3. Obtain an estimate  $\hat{F}_z$  of  $F_z$  (hence an estimate of the ROC curve) as,

$$\hat{F}_z^{(l)}(t) = \frac{1}{S} \sum_{s=1}^S F_{w_s^{(l)}}(t) = \frac{1}{S} \sum_{s=1}^S \frac{1}{w_s^{(l)}} \min\{z, w_s^{(l)}\}, \quad t \in (0, 1). \quad (2.4)$$

4. Given the sample  $\mathbf{w}^{(l)}$ , we can also obtain  $\widehat{AUC}^{(l)} = \frac{1}{2S} \sum_{s=1}^S (1 - w_s^{(l)})$ .

There are several ways to specify  $G$ . Parametrically, we can specify  $G \sim N(\mu, \sigma^2)$  to propose a parametric representation of the concave ROC curve model (called pCN thereafter)

$$\begin{aligned} z_i | w_i &\sim U(0, w_i), \\ \eta^{-1}(w_i) &\sim N(\mu, \sigma^2). \end{aligned} \quad (2.5)$$

Alternatively, we can propose a semiparametric way of modeling  $G$  to allow more flexibility. By following a DPM modeling approach (Sethuraman, 1994), we specify

$$\begin{aligned} G(w_i | \mu_i, \sigma^2) &= \int K(w_i; \mu_i, \sigma^2) dH(\mu_i), \\ H(\mu_i) &\sim \mathcal{D}(\alpha H_0(\mu_i)), \end{aligned}$$

where  $\mathcal{D}$  denotes a Dirichlet process (Ferguson, 1973) with base measure  $H_0$  and precision parameter  $\alpha$  and  $K(\cdot; \mu, \sigma^2)$  is a kernel with parameters  $\mu$  and  $\sigma$ . Following the parametric

approach of concavity modeling, we can write our semi-parametric concave model (called spCN thereafter) using DPM prior for  $G$  as:

$$\begin{aligned} z_i | w_i &\sim U(0, w_i), \\ \eta^{-1}(w_i | \mu_i, \sigma^2) &\sim G(w_i | \mu_i, \sigma^2) = \int K(w_i; \mu_i, \sigma^2) dH(\mu_i), \\ K(w; \mu_i, \sigma^2) &= N(w_i | \mu_i, \sigma^2), \\ H(\cdot) &\sim \mathcal{D}(\alpha_0 H_0(\cdot)), \\ H_0(\mu_i) &= N(\mu_i | \mu_0, \sigma_0^2), \end{aligned}$$

where  $\alpha_0, \mu_0, \sigma_\mu^2$  are all constants. Equivalently, this spCN model can be written follows:

$$\begin{aligned} z_i | w_i &\sim U(0, w_i), \\ \eta^{-1}(w_i | \mu_i, \sigma^2) &\sim N(\mu_i, \sigma^2), \\ \mu_i | H &\sim H = \sum_k p_k \delta_{\mu_k^*}, \\ p_1 = V_1, p_k &= V_k(1 - V_{k-1}) \cdots (1 - V_1), \\ V_i &\sim \text{Beta}(1, \alpha), \\ \mu_i^* &\sim H_0 = N(\mu_0, \sigma_0^2). \end{aligned} \tag{2.6}$$

## 2.4 Estimation, inference, and computation

We take a Bayesian approach for the inference and use proper objective prior. Specifically, each  $\mu_i$  follows  $N(0, 100)$  priors and variance parameter  $\sigma^2$  follows  $IG(0.01, 0.01)$ .

We use **RJAGS** to implement the Monte Carlo Markov chain (MCMC) algorithms to generate samples from the posterior distribution of the model parameters given the data. Both visual inspection of the trace plots and diagnostic tools ([Gelman et al., 1992](#)) are used to ensure convergence of the MCMC chains. After convergence, we thin the iterations to produce a sample of 5000 to produce posterior means, standard deviations and 95% credible intervals. R code of implementing simulation and real data analysis will be made available online.

## 3 Simulation studies

As PV-based models have been studied elsewhere ([Ghosal and Chen, 2022](#); [Chen and Ghosal, 2021](#); [Stanley and Tubbs, 2018](#); [Ghosal et al., 2022](#); [Pepe and Cai, 2004](#)), we focus on the concave ROC curves in our simulations. We generate data from Binormal (PBN), Bigamma (BG), and pCN and evaluate the performance of existing and proposed approaches. We examine bias and efficiency in AUC estimates and empirical mean square error (EMSE) in ROC curve estimates, where

$$EMSE = \int_0^1 \left[ \widehat{ROC}(t) - ROC(t) \right]^2 dt.$$

EMSE is the preferred metric of performance since ROC curves with different curvatures can have the same AUC value.

### 3.1 Simulation scenarios

1. **Proper Bi-Normal (PBN)**. We generate the reference ( $Y^0$ ) and affected ( $Y^1$ ) test scores respectively from  $Y^0 \sim N(0, 1)$  and  $Y^1 \sim N\left(\frac{\alpha_0}{\alpha_1}, \frac{1}{\alpha_1^2}\right)$ . Following the equivalence of PBN and the bi-chi-square distribution (Hillis, 2016), we calculate  $\lambda$  and  $\theta$  as

$$\lambda = \frac{1}{\alpha_1^2} \text{ and } \theta = \frac{\alpha_0^2 \alpha_1^2}{(1 - \alpha_1^2)^2},$$

so that the true ROC curve and corresponding AUC can be obtained as

$$ROC(t) = \begin{cases} 1 - F_{\lambda\theta}\left(\frac{1}{\lambda}F_{\theta}^{-1}(1-t)\right), & \lambda > 1 \\ F_{\lambda\theta}\left(\frac{1}{\lambda}F_{\theta}^{-1}(1t)\right), & \lambda < 1 \end{cases} \quad (3.1)$$

$$AUC = \Phi\left(\frac{\sqrt{\theta}\sqrt{\lambda-1}}{\sqrt{\lambda+1}}\right) + 2F_{BVN}\left(-\frac{\sqrt{\theta}\sqrt{\lambda-1}}{\sqrt{\lambda+1}}, 0; -\frac{2\sqrt{\lambda}}{\lambda+1}\right), \quad (3.2)$$

where  $F_{\nu}$  is then CDF of a chi-square distribution with noncentrality parameter  $\nu$  and  $F_{BVN}(\cdot, \cdot; \rho)$  denotes the CDF of a standardized bivariate normal distribution with correlation  $\rho$ . The case of  $\lambda = 1$ , the true AUC and ROC have the same forms as that from the Bi-Normal (BN) model:  $AUC = \Phi\left(\frac{\alpha_0}{\sqrt{1+\alpha_1^2}}\right)$ ,  $ROC(t) = \Phi(\alpha_0 + \alpha_1\Phi^{-1}(t))$ .

2. **Bi-Gamma (BG)**: The BG model (Dorfman et al., 1996) postulates that  $Y^0 \sim Gam(k, \phi_0)$  and  $Y^1 \sim Gam(k, \phi_1)$ , where  $Gam(k, \phi)$  denotes a gamma distribution with mean  $k\phi$ . True ROC and AUC are given by

$$ROC(t) = 1 - \mathbb{G}_1(\mathbb{G}_0^{-1}(1-t)) \quad (3.3)$$

$$AUC = 1 - H_{(2k, 2k)}\left(\frac{\phi_0}{\phi_1}\right), \quad t \in (0, 1). \quad (3.4)$$

where  $\mathbb{G}_l(\cdot)$  is the CDF of  $Gam(k, \phi_l)$ ,  $l = 0, 1$ , and  $H_{\nu_1, \nu_2}$  is CDF of the F-distribution with degrees of freedom  $\nu_1$  and  $\nu_2$ .

3. **Parametric Concave (pCN)**: The third data-generating scenario follows from the proposed pCN model. We first generate the healthy score  $Y^0 \sim N(0, 1)$  then the PV  $z \sim U(0, \Phi^{-1}(w^*))$ , where  $w^*$  is from  $N\left(\frac{\alpha_0}{\alpha_1}, \frac{1}{\alpha_1^2}\right)$ . Assuming normality on the reference population scores, the affected scores can be calculated as  $Y^1 = \Phi^{-1}(1 - z)$ . Since the AUC and ROC curve do not have closed forms under pCN, we take an empirical approach to obtain their truth. In particular, we first obtain  $z$  and then calculate its empirical CDF and corresponding  $AUC = 1 - \bar{z}$ . We replicate this process 10000 times and treat the average of empirical CDFs and AUCs as the underlying truth.

We vary the underlying parameters of each of the three data-generating mechanisms to obtain three levels of AUC: low, medium, and high. Under PBN, the AUC level is low with

AUC of 0.673 ( $\alpha_0 = 0.5, \alpha_1 = 0.7$ ), medium with AUC of 0.762 ( $\alpha_0 = 0.5, \alpha_1 = 0.45$ ) and high with AUC of 0.842 ( $\alpha_0 = 0.5, \alpha_1 = 0.28$ ). Under BG, the corresponding true AUCs are 0.665 ( $k = 1, \phi_0 = 1, \phi_1 = 2$ ), 0.774 ( $k = 1, \phi_0 = 1, \phi_1 = 3.5$ ) and 0.869 ( $k = 1, \phi_0 = 1, \phi_1 = 7$ ). Similarly, when the data are generated from the pCN model, the corresponding AUCs are 0.619 ( $\alpha_0 = 1, \alpha_1 = 1$ ), 0.741 ( $\alpha_0 = 0.1, \alpha_1 = 3$ ) and 0.916 ( $\alpha_0 = -15, \alpha_1 = 15$ ). For each of these nine combinations, we generate test scores for reference ( $N = 1000$ ) and affected ( $N = 1000$ ) subjects and fit five fitting models to the resultant data: BN, BG, PBN, pCN, and spCN.

We create 1000 data replicates and report average posterior mean and bias of AUC and EMSE (times 1000) of ROC in Table 1. We also plot 200 randomly selected estimated ROC curves from the 1000 replicated datasets in Figures 2-4.

### 3.2 Simulation results

When the data generating mechanism is PBN, the EMSE is lowest for the PBN fitting model across the three levels of AUCs, an expected outcome since the model fitting model is correctly specified. The proposed semiparametric model spCN achieves the second lowest EMSE, followed by the parametric concave model pCN. BG produces highest EMSE in estimating ROCs and highest bias in estimating AUCs. BN model also produces high bias in AUC and non-concave ROCs as illustrated in the first column of Figure 2.

When data are generated from the BG model, the BG model itself is unbiased in estimating AUC and produces the lowest EMSEs in estimating ROC curves. Similar to the previous scenario, the semiparametric model spCN consistently has superior EMSEs compared to other models across varying levels of AUC. Similarly, the performance of the pCN model closely trailed that of the spCN model. However, in this scenario, the PBN model performs poorly both in terms of bias in estimating AUCs and EMSE in estimating ROCs.

Finally when the data generating mechanism is pCN, the pCN model itself is unbiased and yields the smallest EMSEs. The semiparametric model spCN has almost identical performance to the pCN model. On the other hand, the PBN model performs poorly except when the AUC level is low. Figures 2-4 reflect these observations.

In summary, if the goal is to estimate ROC curves that are proper in the sense of satisfying optimal decision theory, it is preferred to apply the proposed semiparametric or parametric PV-based concave ROC approaches. Existing concave ROC approaches such as PBN and BG may have similar or slightly better performance when we know the true underlying models, the fact that we never possess such knowledge makes them less desirable. As popular as it is, the BN model will not guarantee ROC curves estimates that are proper.



Table 1: Simulation results

Generating Model		Fitting model	True AUC	Mean	Bias	EMSE $\times 1000$
Model	AUC level					
PBN	Low	BN	0.673	0.656	-0.017	0.532
		BG	0.673	0.646	-0.027	2.733
		PBN	0.673	0.675	0.002	0.120
		pCN	0.673	0.661	-0.012	0.814
		spCN	0.673	0.666	-0.007	0.328
	Medium	BN	0.762	0.672	-0.089	8.789
		BG	0.762	0.665	-0.097	18.293
		PBN	0.762	0.766	0.004	0.068
		pCN	0.762	0.699	-0.062	5.976
		spCN	0.762	0.728	-0.033	1.564
	High	BN	0.842	0.682	-0.160	26.604
		BG	0.842	0.674	-0.167	49.171
		PBN	0.842	0.847	0.006	0.033
		pCN	0.842	0.730	-0.112	17.542
		spCN	0.842	0.768	-0.074	7.256
BG	Low	BN	0.665	0.674	0.009	4.656
		BG	0.665	0.665	0.000	0.118
		PBN	0.665	0.744	0.079	9.192
		pCN	0.665	0.651	-0.014	0.749
		spCN	0.665	0.664	-0.001	0.297
	Medium	BN	0.774	0.776	0.002	5.290
		BG	0.774	0.774	0.000	0.091
		PBN	0.774	0.864	0.090	12.629
		pCN	0.774	0.767	-0.007	0.689
		spCN	0.774	0.773	-0.001	0.277
	High	BN	0.869	0.879	0.010	2.573
		BG	0.869	0.869	0.000	0.054
		PBN	0.869	0.938	0.068	7.272
		pCN	0.869	0.884	0.014	0.692
		spCN	0.869	0.863	-0.006	0.322
pCN	Low	BN	0.619	0.620	0.002	0.225
		BG	0.619	0.610	-0.009	0.924
		PBN	0.619	0.622	0.003	0.216
		pCN	0.619	0.618	-0.001	0.215
		spCN	0.619	0.618	-0.001	0.216
	Medium	BN	0.741	0.743	0.002	0.799
		BG	0.741	0.715	-0.026	8.116
		PBN	0.741	0.754	0.013	1.225
		pCN	0.741	0.741	0.000	0.188
		spCN	0.741	0.741	0.000	0.189
	High	BN	0.916	0.913	-0.003	1.206
		BG	0.916	0.857	-0.060	14.106
		PBN	0.916	0.922	0.006	1.648
		pCN	0.916	0.916	0.000	0.182
		spCN	0.916	0.916	0.000	0.184

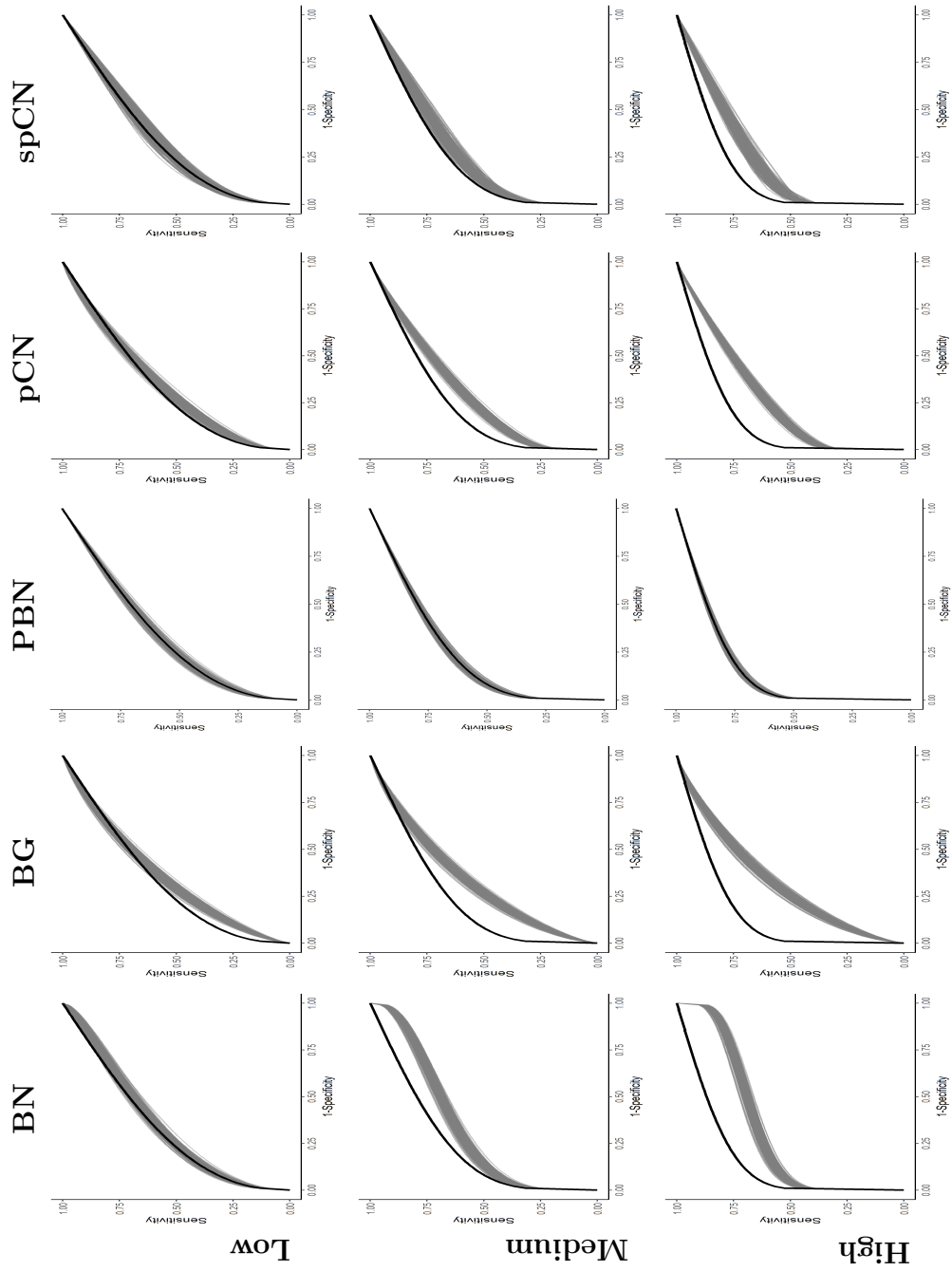


Figure 2: ROC estimates for case when data is generated from PBN model

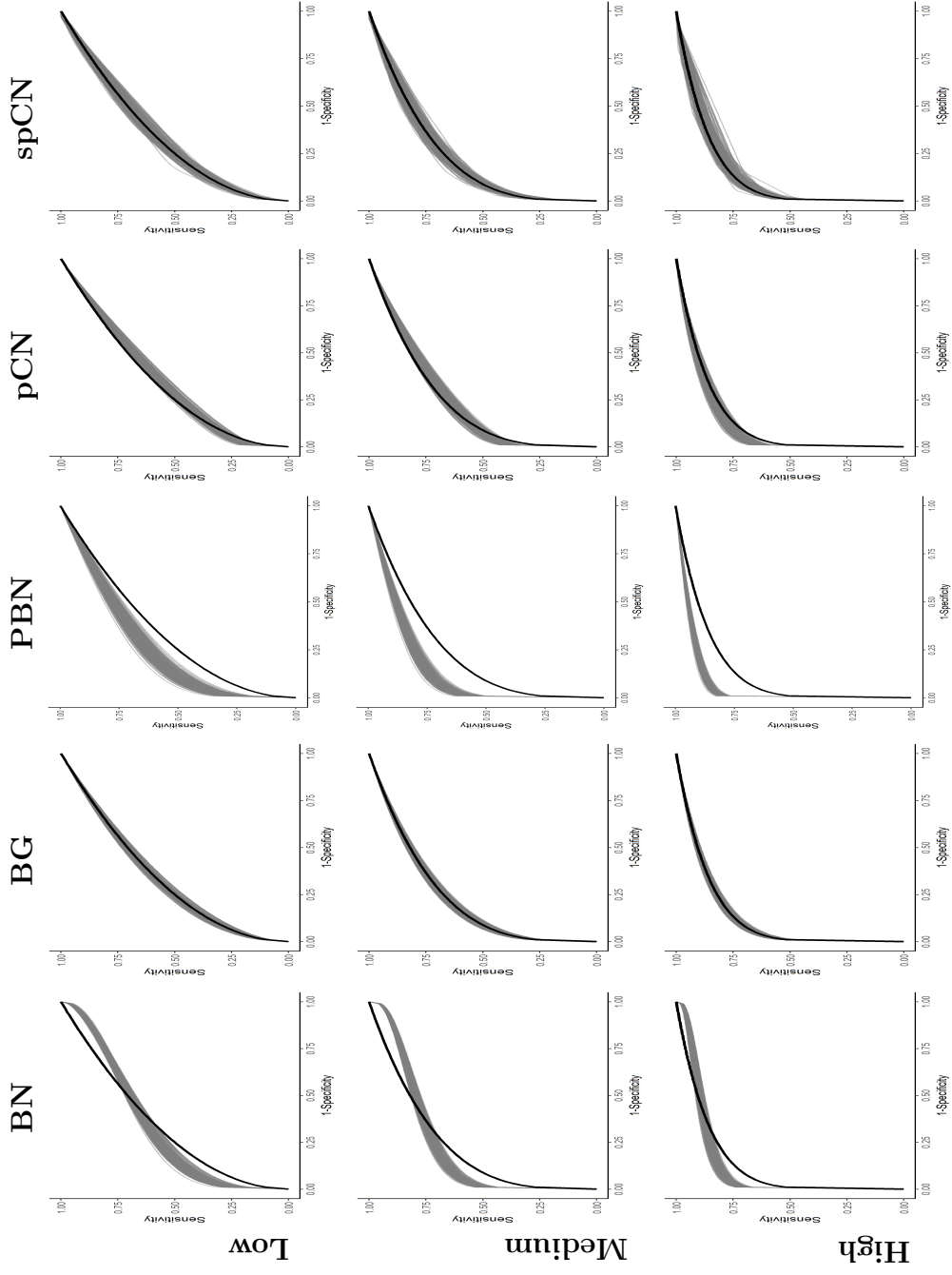


Figure 3: ROC estimates for case when data is generated from BG model

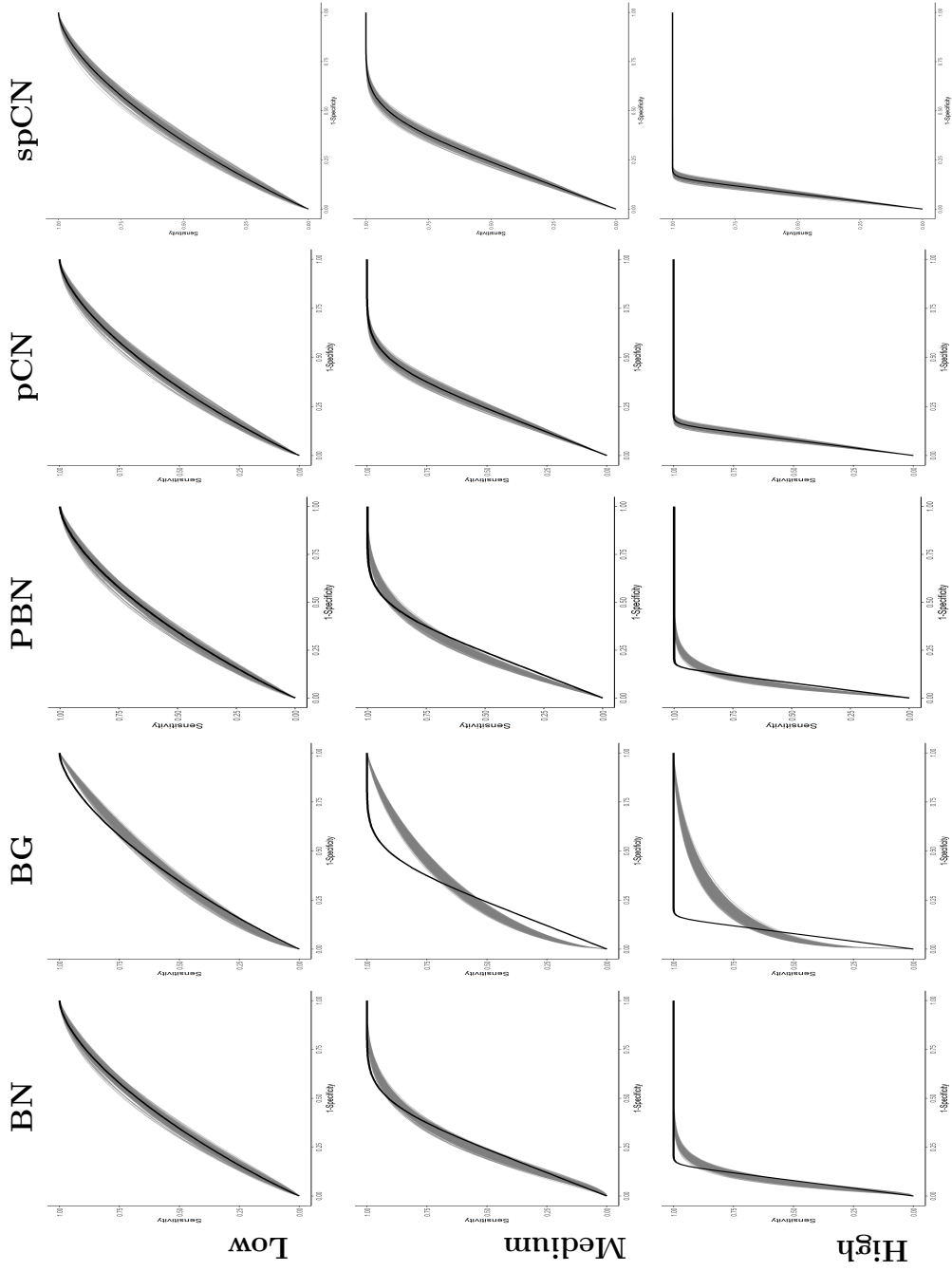


Figure 4: ROC estimates for case when data is generated from pCN model

## 4 Application

### 4.1 Pancreatic cancer data

For application and illustration, we use the pancreatic cancer data that was studied by the Mayo Clinic. The study aimed to compare the diagnostic assessments of carbohydrate antigen (CA199) and cancer antigen (CA125) in screening for pancreatic cancer. More on this can be found in [Wieand et al. \(1989\)](#).

In the data application, we are only interested in the CA199 marker. Figure 5 has the densities and summary of the log-transformed CA199 marker. Briefly, levels of carbohydrate antigen (CA199) marker of 90 affected (with pancreatic cancer) and 51 reference subjects are used to estimate the ROC curve for discriminating pancreatic cancer. The means (standard deviations) of the logarithm of CA199 marker are 2.472 (0.865) in the reference group and 5.415 (2.342) in the affected group.

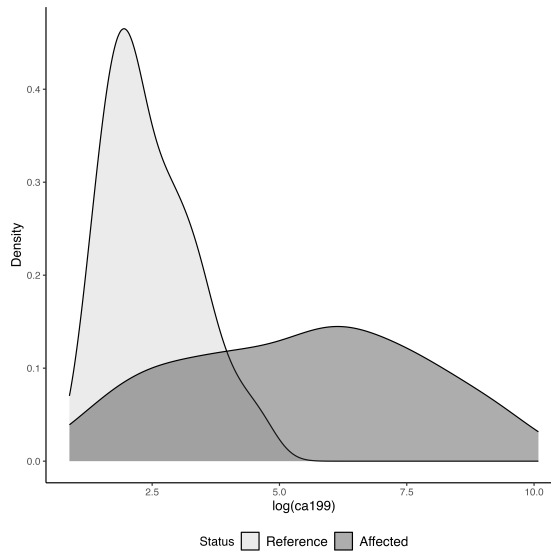


Figure 5: Summary of the pancreatic cancer data

### 4.2 Data analysis

We fit BN, BG, PBN, pCN and spCN models to the pancreatic cancer data. For the parametric pCN model, we take a logarithmic transformation and model  $\log(Y^0)$  as follows:

$$\log(Y_i^0) = \alpha_0 + e_{i'}, e_{i'} \sim N(0, \sigma_0^2). \quad (4.1)$$

Then the PV  $z_i$  are calculated under the parametric approach as

$$z_i = 1 - \Phi \left( \frac{\log(y_i^1) - \hat{\alpha}_0}{\hat{\sigma}_0} \right).$$

For the semiparametric approach, the PV is computed after estimating the distribution of the affected scores using DPM as

$$z_i = 1 - \sum_{k=1}^H \pi_k \Phi \left( \frac{\log(y_i^1) - \hat{\mu}_k}{\hat{\sigma}_0} \right).$$

Once we have estimated the PV, we model  $z_i$  parametrically as

$$\begin{aligned} z_i | w_i &\sim U(0, w_i), \\ \eta^{-1}(w_i | \beta_0) &= \beta_0 + \epsilon_{1i}, \\ \epsilon_{1i} &\sim N(0, \sigma^2), \quad i = 1, \dots, N. \end{aligned}$$

The semiparametric concave model follows the same as (2.6).

We estimate ROC and AUC as discussed in equation (2.4) and tabulate the posterior mean AUC estimates and 95% credible interval in Table 2 under different models. The corresponding ROC curves are shown in Figure 6.

Table 2: Posterior mean AUC estimates and 95% credible interval (CI) for Pancreatic cancer data.

Model	Mean	95% CI
BN	0.872	(0.842, 0.899)
BG	0.881	(0.849, 0.908)
PBN	0.900	(0.883, 0.917)
pCN	0.882	(0.850, 0.910)
spCN	0.855	(0.803, 0.903)

Based on the AUC estimates Table 2 and ROC curves in Figure 6 produced by different models, we infer high diagnostic accuracy for the biomarker CA199 in screening for pancreatic cancer population (mean AUC ranging from 0.86 - 0.90). In Table 2, we see a reasonable difference in the AUC estimates from different models. Although BN produces an AUC estimate similar to the other four models, estimate of the ROC curve under it is clearly nonconcave (Figure 6 (a)). Among the four concave ROC models, PBN produces an AUC estimate with the narrowest 95% credible interval. It is interesting to see the posterior mean AUC is smallest under SpCN; its wide 95% credible interval could be a result of small sample size.

## 5 Discussion

In this paper, we have proposed a PV-based framework where to impose concavity curvature on ROC curves. This was achieved by utilizing the connection between cumulative distribution function of the placement value of a test score and a ROC curve. Compared

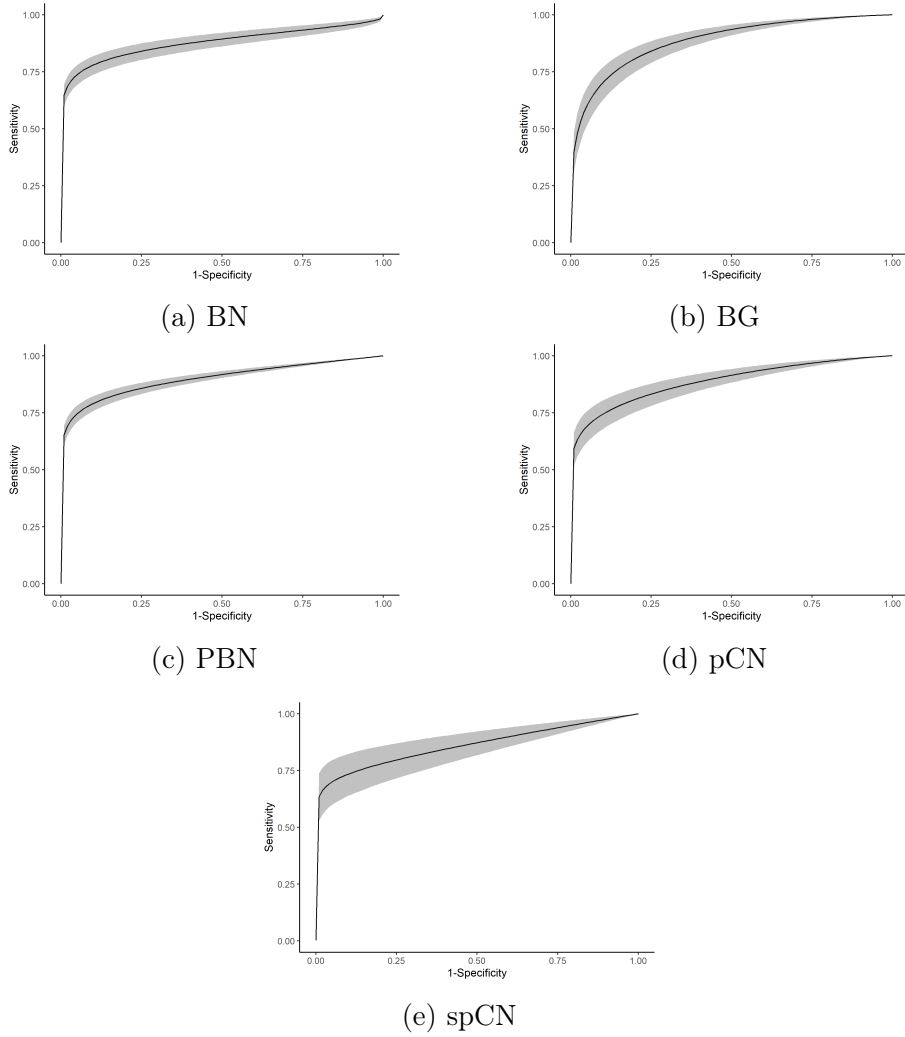


Figure 6: Estimated ROC curves under different models for the Pancreatic cancer data.

to existing concave ROC approaches in the literature, the proposed methodology is more flexible and can better accommodate different distributional features. Our simulation study results suggest that the proposed semiparametric concave approach achieves better accuracy in AUC and ROC estimates in different scenarios, followed by its parametric counterpart. This work provides a new useful tool in diagnostic accuracy analysis, especially when strong parametric distributional assumptions are not supported.

Other forms of constraints have been considered in ROC curve analysis. For example, Ghosal and Chen (2022) introduced a PV-based BN model that allows for multiple ROC curves with AUC ordering constraint. One natural future research direction is to jointly consider shape- and order-constrained multiple ROC curves, in the sense that several ROC curves are ordered (e.g., in AUC) and each individual one is concave. One immediate challenge is the development of efficient computational algorithms, as the multitude of constraints compresses the support of joint posterior distribution which is then difficult to sample from.

As another future direction, we can consider accounting for covariates in the ROC framework which will allow us to estimate the covariate-specific or covariate-adjusted concave ROC curves. Covariate adjustment in the concave ROC framework has never been explored and the PV-based framework potentially provides an attractive platform to account for covariates.

## Acknowledgements

This research was supported by the Intramural Research Program of *Eunice Kennedy Shriver* National Institute of Child Health and Human Development. This work utilized the computational resources of the NIH HPC Biowulf cluster. (<http://hpc.nih.gov>)

## References

- Bandos, A. I., Guo, B., and Gur, D. (2017). Estimating the area under roc curve when the fitted binormal curves demonstrate improper shape. *Academic Radiology*, 24(2):209–219.
- Birdsall, T. G. (1966). *The theory of signal detectability: ROC curves and their character*. University of Michigan.
- Cai, T. (2004). Semi-parametric roc regression analysis with placement values. *Biostatistics*, 5(1):45–60.
- Cai, T. and Pepe, M. S. (2002). Semiparametric receiver operating characteristic analysis to evaluate biomarkers for disease. *Journal of the American statistical Association*, 97(460):1099–1107.
- Campbell, G. and Ratnaparkhi, M. V. (1993). An application of lomax distributions in receiver operating characteristic (ROC) curve analysis. *Communications in Statistics-Theory and Methods*, 22(6):1681–1687.



- Chen, Z. and Ghosal, S. (2021). A note on modeling placement values in the analysis of receiver operating characteristic curves. *Biostatistics & Epidemiology*, 5(2):118–133.
- Dorfman, D. D., Berbaum, K. S., Metz, C. E., Lenth, R. V., Hanley, J. A., and Dagga, H. A. (1996). Proper receiver operating characteristic analysis: the bigamma model. *Academic Radiology*, 4(2):138–149.
- Egan, J. P. (1975). *Signal detection theory and ROC-analysis*. Academic press.
- Ferguson, T. S. (1973). A bayesian analysis of some nonparametric problems. *The Annals of Statistics*, pages 209–230.
- Gelman, A., Rubin, D. B., et al. (1992). Inference from iterative simulation using multiple sequences. *Statistical Science*, 7(4):457–472.
- Ghosal, S. and Chen, Z. (2022). Discriminatory capacity of prenatal ultrasound measures for large-for-gestational-age birth: A Bayesian approach to roc analysis using placement values. *Statistics in Biosciences*, 14(1):1–22.
- Ghosal, S., Grantz, K. L., and Chen, Z. (2022). Estimation of multiple ordered roc curves using placement values. *Statistical Methods in Medical Research*, 31(8):1470–1483.
- Green, D. M., Swets, J. A., et al. (1966). *Signal detection theory and psychophysics*, volume 1. Wiley New York.
- Hansen, M. B. and Lauritzen, S. L. (2002). Nonparametric Bayes inference for concave distribution functions. *Statistica Neerlandica*, 56(1):110–127.
- Hillis, S. L. (2012). Simulation of unequal-variance binormal multireader ROC decision data: an extension of the Roe and Metz simulation model. *Academic Radiology*, 19(12):1518–1528.
- Hillis, S. L. (2016). Equivalence of binormal likelihood-ratio and bi-chi-squared ROC curve models. *Statistics in Medicine*, 35(12):2031–2057.
- Hillis, S. L. and Berbaum, K. S. (2011). Using the mean-to-sigma ratio as a measure of the improperness of binormal ROC curves. *Academic Radiology*, 18(2):143–154.
- Lin, H., Zhou, X.-H., and Li, G. (2012). A direct semiparametric receiver operating characteristic curve regression with unknown link and baseline functions. *Statistica Sinica*, 22:1427.
- McClish, D. K. (1989). Analyzing a portion of the ROC curve. *Medical decision making*, 9(3):190–195.
- Metz, C. E. and Pan, X. (1999). “Proper” binormal ROC curves: theory and maximum-likelihood estimation. *Journal of Mathematical Psychology*, 43(1):1–33.
- Mossman, D. and Peng, H. (2016). Using dual beta distributions to create “proper” ROC curves based on rating category data. *Medical Decision Making*, 36(3):349–365.

- Pepe, M. S. (2003). *The statistical evaluation of medical tests for classification and prediction*. Medicine.
- Pepe, M. S. and Cai, T. (2004). The analysis of placement values for evaluating discriminatory measures. *Biometrics*, 60(2):528–535.
- Peterson, W., Birdsall, T., and Fox, W. (1954). The theory of signal detectability. *Transactions of the IRE professional group on information theory*, 4(4):171–212.
- Sacchetto, L. and Gasparini, M. (2018). Proper likelihood ratio based ROC curves for general binary classification problems. *arXiv preprint arXiv:1809.00694*.
- Sethuraman, J. (1994). A constructive definition of dirichlet priors. *Statistica Sinica*, 4(2):639–650.
- Stanley, S. and Tubbs, J. (2018). Beta regression for modeling a covariate adjusted ROC. *Science Journal of Applied Mathematics and Statistics*, 6(4):110.
- Wieand, S., Gail, M. H., James, B. R., and James, K. L. (1989). A family of nonparametric statistics for comparing diagnostic markers with paired or unpaired data. *Biometrika*, 76(3):585–592.